A new critical study of photon production in hadronic collisions

Patrick Aurenche, Michel Fontannaz, Jean-Philippe Guillet, Eric Pilon, Monique Werlen

A NEW CRITICAL STUDY OF PHOTON PRODUCTION IN HADRONIC COLLISIONS

P. Aurenche[1], M. Fontannaz[2], J.Ph. Guillet[1], E. Pilon[1], M. Werlen[1]

1. *Laboratoire d'Annecy-le-Vieux de Physique Théorique LAPTH,* [*]
   B.P. 110, F-74941 Annecy-le-Vieux Cedex, France

2. *Laboratoire de Physique Théorique LPT,* [†]
   Bât. 210, Université de Paris-Sud, F-91405 Orsay Cedex, France

Abstract

In the light of the new prompt photon data collected by PHENIX at RHIC and by D∅ at the run II of the Tevatron, we revisit the world prompt photon data, both inclusive and isolated, in hadronic collisions, and compare them with the NLO QCD calculations implemented in the Monte Carlo programme `JETPHOX`.

1   Introduction

Two experiments have recently collected prompt photon data. For the first time, a collaboration (PHENIX at $\sqrt{s}$ = 200 GeV at RHIC) has been able to collect data both for the inclusive [1] and the isolated case [2] which should help better understand the role of the fragmentation component in prompt photon production. Furthermore, during run II of the Tevatron ($\sqrt{s}$ = 1.96 GeV), the DØ collaboration [3] has measured isolated prompt photons whose transverse momenta p_T range from 23 to about 300 GeV, the widest domain ever covered. These new experimental results shed some light on a controversy which has been plaguing prompt photon phenomenology since the late 90's.

Indeed, many years of intense experimental efforts, ranging from fixed targets [4, 5, 6, 7, 8, 9, 10, 11] to colliders [12, 13, 14, 15, 16, 17], have led to a wealth of experimental data on prompt photon production in hadronic collisions, but also to a controversial situation. In particular, in the late 90's some confusion was created by one fixed target experiment [9] which found cross sections several times above theoretical predictions based on Next-to-Leading Order (NLO) calculations; data and theory disagreed both in magnitude and shape. This disagreement triggered a debate on large recoil effects possibly of non perturbative origin. The resummation of threshold as well as recoil effects induced by soft gluon radiation in the single particle inclusive cross sections have been performed. In the meantime, full NLO calculations have been implemented in more flexible Monte Carlo programmes at the partonic level. Programmes of this type account for experimental cuts in an easy way, match naturally the binning of experimental data and, by histogramming of the partonic configurations generated, allow for a straightforward study of correlations. The latter provide more constrained and refined tests of the short distance dynamics than the single particle inclusive distributions.

In the present article we propose a reexamination of prompt photon data in the light of these new experimental results. In section 2 we formulate the theoretical framework of our study, and discuss the complementary features of dedicated resummed calculations and NLO calculations implemented in Monte carlo programmes such as JETPHOX [18] used in the present study. In section 3, we present a comparison of this theoretical framework with the new PHENIX data, and with the new DØ data. We then reexamine the older world data in the light of this comparison. Section 4 contains our conclusions.

2   Theoretical framework and ambiguities

2.1   Mechanisms of production of prompt photons

Schematically, the production of a prompt photon proceeds via two mechanisms. In the first one, which may be called 'direct' (D), the photon behaves as a high p_T colourless parton, i.e. it takes part in the hard subprocess, and it is most likely to be well separated from any hadronic environment. In the other one, which may be called 'fragmentation' (F), the photon behaves as a kind of (anomalous) hadron, i.e. it results from the collinear fragmentation of a coloured high p_T parton, and is it most probably accompanied by hadrons - unless the photon carries away most of the transverse momentum of the fragmenting parton, which is usually the situation in fixed target experiments.

From a technical point of view, (F) emerges from the calculation of the higher order corrections to (D) in the perturbative expansion in powers of the strong coupling α_s. At higher orders, final state multiple collinear singularities appear in any subprocess where a high p_T parton of species k (quark or gluon)

1

undergoes a cascade of successive collinear splittings ending up with a splitting into a photon. These singularities are factorised to all orders in α_s according to the factorisation theorem, and absorbed into fragmentation functions of parton k to a photon, $D_{\gamma/k}(z, M_F)$, defined in some arbitrary fragmentation scheme, at some arbitrary fragmentation scale M_F. The point-like coupling of the photon to quarks is responsible for the well-known anomalous behaviour of $D_{\gamma/k}(z, M_F)$, roughly as $\alpha_{em}.\alpha_s^{-1}(M_F)$ when the fragmentation scale M_F, chosen of the order of a hard scale of the subprocess, is large compared to $\mathcal{O}(1)$ GeV. In this article, (D) is precisely given by the Born term plus the fraction of the higher order corrections from which final state collinear singularities have been subtracted according to the $\overline{\text{MS}}$ factorization scheme. (F) is the contribution involving a fragmentation function of any parton into a photon in the $\overline{\text{MS}}$ factorization scheme. The differential cross section in transverse momentum p_T and rapidity η can thus be written synthetically as:

$$\sigma^\gamma = \sigma^{(D)}(\mu_R, M, M_F) + \sum_{k=q,\bar{q},g} \sigma_k^{(F)}(\mu_R, M, M_F) \otimes D_{\gamma/k}(M_F) \tag{1}$$

where $\sigma_k^{(F)}$ describes the production of a parton k in a hard collision. The arbitrary parameters μ_R, M and M_F are respectively the renormalisation, initial-state factorisation, and fragmentation scales. Let us stress once more that the splitting between (D) and (F) is arbitrary: it relies on a choice of factorisation scheme and scale to which refer the definitions of each of these contributions. In particular, both (D) and (F) depend on M_F, so that the partial cancellation of the M_F dependence in the predictions proceeds in a qualitatively different, and quite more complicated, way here than in the purely hadronic case. The dependence of the NLO predictions with respect to μ_R, M and M_F will be discussed in sect. 3. When all scales are taken to be equal, they will be noted μ.

The study provided in this article relies on the calculation of both (D) and (F) at next-to-leading order (NLO) accuracy [18], which takes the form (η is the photon rapidity)

$$\frac{d\sigma}{d\vec{p}_T d\eta} = \frac{d\sigma^{(\text{D})}}{d\vec{p}_T d\eta} + \frac{d\sigma^{(\text{F})}}{d\vec{p}_T d\eta} \tag{2}$$

where

$$\frac{d\sigma^{(\text{D})}}{d\vec{p}_T d\eta} = \sum_{i,j=q,\bar{q},g} \int dx_1 dx_2 \, F_{i/h_1}(x_1, M) \, F_{j/h_2}(x_2, M) \frac{\alpha_s(\mu_R)}{2\pi} \left(\frac{d\hat{\sigma}_{ij}}{d\vec{p}_T d\eta} + \frac{\alpha_s(\mu_R)}{2\pi} K_{ij}^{(\text{D})}(\mu_R, M, M_F) \right) \tag{3}$$

and

$$\begin{aligned}
\frac{d\sigma^{(\text{F})}}{d\vec{p}_T d\eta} &= \sum_{i,j,k=q,\bar{q},g} \int dx_1 dx_2 \frac{dz}{z^2} \, F_{i/h_1}(x_1, M) \, F_{j/h_2}(x_2, M) \, D_{\gamma/k}(z, M_F) \\
&\qquad \left(\frac{\alpha_s(\mu_R)}{2\pi} \right)^2 \left(\frac{d\hat{\sigma}_{ij}^k}{d\vec{p}_T d\eta} + \frac{\alpha_s(\mu_R)}{2\pi} K_{ij,k}^{(\text{F})}(\mu_R, M, M_F) \right)
\end{aligned} \tag{4}$$

where $F_{i/h_{1,2}}(x, M)$ are the parton distribution functions of parton species i inside the incoming hadrons $h_{1,2}$, at momentum fraction x and factorisation scale M; $\alpha_s(\mu_R)$ is the strong coupling defined in the $\overline{\text{MS}}$ renormalisation scheme at the renomalisation scale μ_R. The knowledge of $\Lambda_{\overline{MS}}$, e.g. from deep-inelastic scattering experiments, completely specifies the NLO expression of the running coupling $\alpha_s(\mu_R)$. The NLO correction terms to (D) and (F), $K_{ij}^{(\text{D})}$ [19, 20] and $K_{ij,k}^{(\text{F})}$ [21] respectively, are known and their expressions in the $\overline{\text{MS}}$ scheme will be used. The dependence of these functions on the kinematical variables $x_1, x_2, z, \sqrt{s}, p_T$ and η has not been explicitly displayed. The structure

2

and fragmentation functions have been determined at the required level of accuracy by NLO fits to the data.

The results of the NLO calculation of (D) have been known for a long time [19]. They were first implemented in computer codes in a form dedicated to one particle inclusive distributions, the integration over the phase space variables being done analytically. As such, these codes were fast but not flexible enough to account for the various experimental selection and, especially, the isolation cuts used at colliders, and they were not suited to study correlations. The calculation has been subsequently implemented using a 'Monte Carlo' method [22] which however included the (F) contribution only at leading order (LO) accuracy. The calculation of the NLO corrections to (F) became also progressively available along the same steps [21, 23, 18]. The present study relies on the implementation of the NLO calculation of both (D) and (F) in a Monte Carlo programme*, called `JETPHOX`, briefly described in subsect. 2.3.

More recently, expressions involving the resummation, at next-to-leading logarithmic (NLL) accuracy of terms which are logarithmically large at the phase space boundary ($x_T = 2p_T/\sqrt{s} \to 1$) have been obtained, first in (D) [24, 25, 26, 27, 28], and more recently in (F) as well [29]. This resummation is performed only for inclusive p_T distributions integrated over all rapidities. The effect of this resummation extends down to values of $x_T \geq$ a few 10^{-1} and thus covers the range of fixed target experiments. They provide a much reduced μ_R and M dependence than with the NLO approximation. The NLO results roughly agree with the resummed calculation in the region populated by fixed target data, when μ_R and M are chosen $\sim p_T/2$ in the former. As for collider experiments, these resummations do not have much impact on the phenomenology in the x_T range $\sim 10^{-2}$ to 10^{-1} covered by the data. The impact of resumming logarithmically enhanced terms at small x_T might be more relevant in the smaller x_T range, yet a proper resummation of this kind has not been studied so far in prompt photon production, to our knowledge.

Even more recently, a joint summation of both threshold and recoil effects due to soft multigluon emission has been performed in [30]. Recoil effects are logarithmically enhanced order by order in the α_s expansion of the q_T distribution of a pair γ-jet; however this logarithmic enhancement is washed out by the integration over the jet when passing to the single photon inclusive p_T distribution. The joint summation recently performed confirmed that this order by order conclusion also holds in the all order resummed result when resummation is performed *before* the integration over the recoiling jet, leaving un-enhanced contributions only, whose effects remain small. The joint summation makes also contact with possible non perturbative effects of k_T kick which are not accounted for in any fixed order calculation. However these non perturbative recoil effects, which are to a large extend unconstrained by theory so far, remain small unless large non perturbative parameters are used; one experiment only argues in favour of such unexpectedly large parameters. This issue will be discussed in sect. 3.

All these resummed calculations have to be performed in a space conjugate to the physical phase space through a Mellin/Fourier transform in order to put the kinematical constraints into a factorisable form. So far they are performed analytically, requiring a dedicated calculation. They cannot easily cop with the various cuts required by experiments, contrarily to the NLO calculation implemented with a Monte Carlo method. Up to now, the use of a NLO Monte Carlo programme in prompt photon phenomenology, supplied by motivated scale choices is still legitimate.

---

*For inclusive observables involving no isolation cuts, we have also used the much faster NLO programme `INCNLO` [18] implementing analytic expressions of the HO corrections.

2.2 Isolated photons

Whereas the contribution from eq. (4) amounts[†] to roughly a few tens of percent of the contribution from eq. (2) at fixed target energies, it becomes dominant at colliders at least in the lower p_T range. However collider experiments - besides PHENIX at RHIC - do *not* perform inclusive measurements of photons, strictly speaking. In order to strongly suppress the overwhelming background of secondary photons coming from the decays of hadrons, mainly π^0, η, etc., collider experiments require an isolation criterion on the photon candidates. A widely used calorimetric criterion, which has the virtue to be implementable also at the partonic level[‡], is the so-called 'cone criterion': in a cone about the direction of the photon defined in rapidity η and azimutal angle ϕ by

$$(\eta - \eta_\gamma)^2 + (\phi - \phi_\gamma)^2 \leq R^2 \tag{5}$$

the accompanying hadronic transverse energy $E_{T\,had}$ is required to be less than some finite amount:

$$E_{T\,had} \leq E_{T\,max} \tag{6}$$

R and $E_{T\,max}$ being specified by each experiment, $E_{T\,max}$ being given either as a fixed value, or as a fixed fraction ϵ_h of the photon's p_T.

Cross sections for producing such isolated photons have been proven to still fulfill the factorisation property, and are finite to all orders in perturbation theory for non zero R and $E_{T\,max}$ [31]. Isolation through eqs. (5, 6) also reduces the contribution (F), although it does not kill it completely: a fraction survives with $z \geq (1 + \epsilon_h)^{-1}$, which involves the *same* fragmentations functions $D_{\gamma/k}(z, M_F)$ as in the unisolated case. The dependence on the isolation parameters R and $E_{T\,max}$ is consistently included in the expression describing the hard subprocess. At colliders energies the mean value $< z >$ for non isolated photons from fragmentation is fairly smaller[§] than $(1 + \epsilon_h)^{-1}$, so that (F) is quite suppressed by isolation cuts. Let us stress that $E_{T\,max}$ has to be non zero otherwise the calculation of the cross section in perturbative QCD is infrared (IR) divergent order by order in perturbation theory, the (D) contribution involving a term $\sim \alpha_S R^2 \log(p_T/E_{T\,max})$. In practice, no IR sensitivity appears down to fairly low values of $E_{T\,max} \sim 1$ GeV due to the smallness of $\alpha_s R^2$. However, the reliability of the theoretical prediction is jeopardized if the value of $E_{T\,max}$ is nearly saturated by minimum bias hadrons, thus leaving almost no room for radiation from the hard event. Another source of trouble for the NLO calculation is caused by the use of too small a cone size, where the collinear sensitivity would require an all order resummation of large $\log R$ terms: the NLO calculation might not be reliable for $R \leq 0.3$ [31].

It is important to stress that the isolated cross section, measured experimentally, cannot be identified with the direct cross section calculated at the Born level, *i.e.* without any contribution of the fragmentation processes. Indeed, besides the fragmentation piece left over $(z \geq (1+\epsilon_h)^{-1})$ as explained above, higher order terms originating from the non-collinear fragmentation processes contribute to the isolated cross sections. Such terms may be important in some kinematical regions as they correspond

---

[†]This statement depends on the choice of scales, especially of M_F. The order of magnitude given here corresponds to a standard choice $M_F \sim \mathcal{O}(p_T)$.

[‡]Vetoes on charged tracks about the direction of the photon are also used experimentaly, however they cannot be accounted for in a partonic calculation. A detailed description of the final state including full hadronisation would be required.

[§]For example $< z >$ is roughly 0.7 at the Tevatron, and 0.6 or less at the LHC [21], whereas typically $(1 + \epsilon_h)^{-1} \geq 0.8 - 0.9$. On the other hand, notice that, at fixed targets, $< z > \sim 0.9$: in practice photons from fragmentation at fixed targets are scarcely accompanied by hadrons, they are *de facto* isolated.

to new hard processes, not allowed at the lowest order : for example, large terms involving the 3-gluon vertex are possible at higher orders while they are forbidden at the lowest one.

2.3   Brief presentation of JETPHOX

We have implemented all contributions to (D) and (F) up to NLO in the computer package JETPHOX [18]. This code is a general purpose cross section integrator of Monte-Carlo type, designed to calculate both single photon inclusive and photon-jet inclusive cross sections and related correlations, accounting easily for any kind of experimental cut (e.g. on kinematics, isolation) implementable at the partonic level. It is the only available code including both (D) and (F) at NLO in a Monte carlo approach. Details on the principles and implementation of this code can be found in [18, 31]. Let us only sketch them briefly.

The treatment of the infrared (IR) soft and collinear singularities of the partonic transition matrix element combines the phase space slicing [32] and subtraction [33] methods. The slicing of phase space is designed as follows. For a generic partonic subprocess $1 + 2 \to 3 + 4 + 5$ two outgoing partons, say 3 and 4, have a high p_T and are well separated in phase space, while 5, say, can be soft, or collinear to either of the four others. The phase space is sliced using two arbitrary (unphysical) parameters p_{Tm} and R_{Th}, with $p_{Tm} \ll ||\vec{p}_{T\,3,4}||$ and $R_{Th} \ll 1$, in four parts:

- Part I corresponds to $||\vec{p}_{T\,5}|| < p_{Tm}$. This cylinder supports the IR and initial state collinear singularities. It also yields a small fraction of the final state collinear singularities.

- Part II a corresponds to $||\vec{p}_{T\,5}|| > p_{Tm}$, $\vec{p}_{T\,5} \in C_3$, where C_3 is the cone defined by $(y_5 - y_3)^2 + (\phi_5 - \phi_3)^2 \leq R_{th}^2$. It supports the final state collinear singularities when 5 is collinear to 3.

- Part II b is defined in a similar way as II a but with the replacement of 3 by 4. It supports the final state collinear singularities when 5 is collinear to 4.

- Part II c is the remaining region: $||\vec{p}_{T\,5}|| \geq p_{Tm}$, and $\vec{p}_{T\,5} \notin C_3, C_4$.

Collinear and soft singularities, which appear on parts I, II a and II b, are first regularised by dimensional continuation from 4 to $n = 4 - 2\varepsilon$ with $\varepsilon < 0$. Then, the n-dimensional integration over particle 5 is performed analytically over these parts. After combination with the corresponding virtual contributions, the infrared singularities cancel, and the remaining collinear singularities which do not cancel are factorised and absorbed in the parton distribution functions or fragmentation functions. The resulting quantities correspond to pseudo cross sections in which the the "integrated out" parton 5 is unresolved from the remaining four hard partons. The word "pseudo" means that they are not genuine cross sections, namely they are not necessarily positive, and they depend on the arbitrary choice of factorisation scheme¶. Part II c yields no singularity, and is thus treated directly in 4 space-time dimensions. These pseudo cross sections, as well as the transition matrix elements on the part II c, are then used to sample partonic events according to a Monte-Carlo method. Last, these partonic events are projected onto histograms thus providing any desired distribution.

By virtue of the factorisation theorem, the contribution (F) alone also provides the NLO cross sections for inclusive hadron- and associated hadron + jet production, once the parton-to-photon fragmentation

---

¶The $\overline{MS}$ factorisation scheme is used.

functions have been replaced by fragmentation functions of partons to the hadron species considered. The phenomenology of correlations in associated prompt photon + jet and hadron + jet production using JETPHOX will be presented in a future article [34].

3   Comparison with data

All the comparisons between data and NLO calculations provided in this section are made using the parton distribution functions of set CTEQ6M [35] ($\alpha_s(M_Z) = .118$) and the parton-to-photon fragmentation functions of set BFGW (set II) [36]. Whenever the scales μ_R, M and M_F are given a common value, the latter is noted μ. The $\overline{MS}$ scheme is used throughout.

3.1   New data from D$\emptyset$ and PHENIX

We start this section by the analysis of the new data taken by the D$\emptyset$ collaboration [3] during the Tevatron Run II at $\sqrt{s} = 1.96$ TeV. The measured cross section, in the range $23\text{ GeV} < p_T < 300\text{ GeV}$, is for isolated photons and we account for the D$\emptyset$ isolation criterion by requiring that the hadronic transverse energy measured in a cone of radius $R = \sqrt{\Delta\phi^2 + \Delta\eta^2} = 0.4$ around the photon is smaller than 10% of the photon's p_T. Theory and data are compared in Fig. 1 and 2, the theoretical curves being obtained with the inputs specified at the beginning of this section. In Fig. 1, all the scales have been set equal to p_T. We see that the agreement between data and NLO QCD is excellent in the whole p_T-range in which the cross section falls by about five orders of magnitude. A more precise comparison is shown in Fig. 2 for the ratio data/theory calculated with several choices of scales between $p_T/2$ and $2p_T$. The sensitivity to the changes in the common scale μ is of some ± 10 % in the whole p_T-range. Using MRST 2004 [37] instead of CTEQ6M changes the predictions by ± 2 %. The present experimental errors have the size of the variations coming from the scale changes; with this accuracy there is no evidence of any systematic deviation of the theory with respect to data.

Another set of recent - still 'very preliminary' - data is presented by the PHENIX collaboration [1, 2] at RHIC. Measurement are done at $\sqrt{s} = 200$ GeV, an intermediate energy between collider measurements at $\sqrt{s} = 630$ GeV and fixed targets measurement at $\sqrt{s} \leq 40$ GeV which will be discussed below. These data cover the range $4 < p_T < 17$ GeV and correspond to two methods of analysis: a subtraction method in which the π^0 background is identified and subtracted (inclusive prompt photon cross section), and an isolation method. We start with a discussion of the isolated data.

The isolation criterion used by the PHENIX collaboration is fitted to the acceptance of its detector. Photons are detected in the coverage $-.30 \leq \eta \leq .30$ and $-.73 \leq \phi \leq .73$ and the hadronic transverse energy is measured in a cone of radius .5 if it also falls into the region $-.35 \leq \eta \leq .35$, $-\pi/4 \leq \phi \leq \pi/4$. When the hadronic energy is outside the acceptance, it is not taken into account. The fraction of hadronic energy thus observed should be less than 10 % of the photon momentum. This criterion amounts effectively to implementing isolation in a smaller region about the photon and we expect the effect of isolation to be smaller than the one due to the standard procedure when all the energy in the cone is taken into account. The NLO code JETPHOX allows us to study the effect of the PHENIX isolation compared to the standard isolation. The ratios of isolated cross sections over the inclusive one are shown in Fig. 3 where the scale $p_T/2$ is used for the theoretical predictions. First, let us note that the isolation effect is large at low p_T. At larger values of p_T the average value of z increases and

the isolation cut is less effective. Also we note that the PHENIX criterion and the standard one lead to appreciable differences in the predictions, of the order of 10 % at low p_T.

Note that the NLO calculations are performed at the parton level for the QCD hard process and do not account for hadronisation effects which can be large at low pt. Moreover we do not describe the soft underlying event with transverse energy which can also fall into the isolation cone. This contribution may even cut the Born contribution (unaccompanied photon). This effect has been studied by the H1 collaboration in the photoproduction of prompt photons and found to be non negligible [38].

The comparison of the PHENIX isolated cross section with the NLO QCD prediction with the scale $\mu = p_T/2$ is shown in Fig. 4. The theory agrees very well with data within errors (systematic errors are not shown in Fig. 4). A more detailed comparison is performed in Fig. 5 in terms of ratios data/theory calculated for two different choices of scales. The statistical errors are relatively large, of the order of the theoretical uncertainty when varying the common scale from $p_T/2$ to $2p_T$. However, the standard choice $p_T/2$ reproduces the data extremely well over the whole p_T range in which the cross section varies by a factor 10^3.

3.2 Previous world data in the light of the new data from D∅ and PHENIX

As there is some overlap in x_T between these new data and some of the previous ones, in particular in the controversial 0.2 to 0.3 range previously covered by the ISR and E706 experiments, it is interesting to reconsider how the 'world data' is described by theory.

We consider now the inclusive pp and $p\overline{p}$ data coming from the fixed target experiments from WA70 ($\sqrt{s} = 23$ GeV) [6], UA6 ($\sqrt{s} = 24.3$ GeV) [11], E706 ($\sqrt{s} = 31.6$ GeV and 38.8 GeV) [10], from the ISR experiments ($\sqrt{s} = 63$ GeV) R110 [7], R806 [5], AFS [8] and the isolated data from CdF at $\sqrt{s} = 1.8$ TeV [16, 17]. The collider data at $\sqrt{s} = 630$ GeV will be discussed separately. Below we shall also compare the pBe data from the E706 experiment [9] with the more recent pp data of the same experiment [10]. The comparison is done with the scales $\mu = p_T/2$ in terms of ratios data/theory. As explained in section 2.1, such a scale is motivated for the fixed target and ISR range by the recent resummed calculations [24, 25, 26, 28, 29]. The results are shown in Fig. 6 which exhibits the striking agreement between theory and data in the whole x_T range, with the exception of the E706 data[∥]. This last point has been already discussed at length for pBe data in ref. [39]. Here the new features are the new D∅ and PHENIX data which confirms the 'world' agreement between theory and data. We emphazise the very good agreement between theory and the PHENIX inclusive data which confirms that already shown with the isolated data in Figs. 4 and 5. If we disregard the E706 data, there is no evidence for any systematic discrepancy between data and theory. In Fig. 6, the fixed target data are somewhat squeezed by the logarithmic scale. In Fig. 7 we emphasized the fixed target domain by using a linear scale which makes the discrepancy between the E706 data and the other data more obvious. The x_T range from 0.15 to 0.3 is well described all the way from TEVATRON collider data at $\sqrt{s} = 1.96$ TeV down to ISR data at $\sqrt{s} = 63$ GeV. The disagreement cannot be due to the 'low' center of mass energy, ($\sqrt{s} = 31.6$, 38.8 GeV), of the E706 experiment since the WA70 and UA6 fixed target data at even lower energies, $\sqrt{s} = 23$ and 24.3 GeV respectively, (and higher x_T) are in good agreement with theory. Let us note that a reasonably accurate determination of α_s, in good agreement with determinations from other processes,was performed by the UA6 collaboration [40].

[∥]Note that the smallest x_T-values of the E706 data correspond to values of p_T down to 3.5 GeV/c (averaged $p_T \simeq$ 3.73 GeV in the first bin).

Let us continue this 'world' comparison by a comment on the low-x_T part of the CDF data. It has been often claimed [41, 42, 16, 17] that there is a disagreement between data and theory, the latter being unable to explain the rise of the former, a 20 % effect in the ratios of Fig. 6 and 7. Here we would like to point out that the significance of this rise is much reduced when experimental errors and theoretical uncertainties are taken into account. Concerning this last point, the slope in the ratio data/theory depends on the choice of the scales as already noted in [43]. An example is given in Fig. 8 where the ratio data/theory is shown for the scales $\mu_R = p_T$, $M = 2p_T$, $M_F = p_T/2$. The choice yields a slight flattening of the curve.

The comparison with the isolated collider data at $\sqrt{s} = 630$ GeV from UA2 [13], CdF [16] and D∅ [15] are shown in Fig. 9. The errors being rather large, it is difficult to draw any precise conclusion from these results. But within the errors, the agreement data versus theory is good : the CDF data tend to be systematically somewhat above the predictions while the UA2 results tend to be slightly below. The apparent slope effect of the D∅ data, at the lowest values of x_T, is not meaningful when taking into account the large systematic errors. As for UA1 data [12], the large error bars do not constrain the theory very much, and we do not show these data here. One can note however that the corresponding ratios would be above one.

We now turn to a comparison of the recent pp data from the E706 collaboration [10] with the pBe data [9] of the same collaboration. This is done in Fig. 10. We clearly distinguish two domains for the E706 data, one for $x_T \geq .34$ and a second one for lower values of x_T. In the large-x_T domain, the ratio data/theory is approximately flat, or slightly decreasing with an average value close to 1.8. Proton-proton data and proton-Beryllium data are compatible within errors. The problem met here by theory is that of the normalisation. Even the use of a small scale $\mu = p_T/3$ does not reconcile NLO QCD with data [39]. The low-x_T domain is characterized by a marked rise of the ratios, up to 4.5 (at $p_T \simeq 3.73$ GeV) when x_T decreases. Here also pp and pBe data are compatible within errors. NLO QCD cannot explain this rise and another mechanism, the κ_T-enhancement, has been put forward by the E706 collaboration to explain the shape and normalisation of the cross sections. Let us note that no other experiment needs such an enhancement.

We end this section by collecting all available prompt photon cross sections $Ed^3\sigma/dp^3$ (inclusive or isolated) on the same plot and comparing them with theoretical predictions evaluated with the scale $\mu = p_T/2$ (Fig. 11). The data span two orders of magnitude in energy and there is agreement over nine orders of magnitude in the cross sections between theory and experiments. This is comparable to the agreement between theory and D∅ run 2 data for the jet cross section [44] and similarly for CDF data [45]. However the prompt photon data and the jet data do not cover the same kinematical region defined in the ($x_T = 2p_T/\sqrt{s}$, p_T^2) plane (which is the equivalent, for large p_T processes, of the (x, Q^2) plane of deep inelastic scattering) as shown in Fig. 12. The combined data therefore give an extremely strong test of QCD.

4   Conclusions and outlook

Two new direct photon data sets shed a new light on the understanding of such processes within the QCD framework, and they confirm that the $\sqrt{s}$ dependence of the reaction can be properly described within the NLO formalism. Agreement between data and theory from $\sqrt{s} = 23$ GeV to 1.8 TeV is very good over nine orders of magnitude in the cross section.

This is in contrast to the view, based only on data from the E706 experiment, that the direct photon

data cannot be understood in the NLO QCD framework without resorting to a non perturbative 'k_T kick'. Indeed, although refinements like resummed calculations have been important to reduce the theoretical uncertainties, they have not permitted to reconcile one data set (namely E706) with theory without using large non perturbative parameters. Such parameters are not needed by other experiments.

Acknowledgments

References

[1] S. S. Adler *et al.* [PHENIX Collaboration], Phys. Rev. D **71** (2005) 071102 [arXiv:hep-ex/0502006].

[2] K. Okada [PHENIX Collaboration], arXiv:hep-ex/0501066.

[3] V.M. Abazov *et al.*, [DØ collaboration], subm. to Phys. Lett. B., Fermilab-Pub-05/523-E, [arXiv:hep-ex/0511054].

[4] M. McLaughlin *et. al.* [E629 collaboration], Phys. Rev. Lett. **51** (1983) 971;
J. Badier *et. al.* [NA3 collaboration], Zeit. für Physik C **31** (1986) 341;
C. De Marzo *et. al.* [NA24 collaboration], Phys. Rev. D **36** (1987) 8;
A.L.S. Angelis *et. al.* [R108 collaboration], Nuc Phys. B **263** (1986) 228

[5] E. Anassontzis *et al.* [R806 Collaboration], Z. Phys. C **13** (1982) 277.

[6] M. Bonesini *et al.* [WA70 Collaboration], Z. Phys. C **37** (1988) 535.

[7] A. L. S. Angelis *et al.* [CMOR Collaboration], Nucl. Phys. B **327** (1989) 541.

[8] T. Åkesson *et al.* [Axial Field Spectrometer Collaboration], Sov. J. Nucl. Phys. **51** (1990) 836 [Yad. Fiz. **51** (1990) 1314].

[9] L. Apanasevich *et al.* [E706 collaboration], Phys. Rev. Lett. **81** (1998) 2642.

[10] L. Apanasevich *et al.* [E706 Collaboration], Phys. Rev. D **70** (2004) 092009 [arXiv:hep-ex/0407011].

[11] G. Ballocchi *et al.* [UA6 Collaboration], Phys. Lett. B **436** (1998) 222.

[12] C. Albajar *et al.* [UA1 Collaboration], Phys. Lett. B **209** (1988) 385.

[13] J. Alitti *et al.* [UA2 Collaboration], Phys. Lett. B **288** (1992) 386.

[14] B. Abbott *et al.* [D0 Collaboration], Phys. Rev. Lett. **84** (2000) 2786 [arXiv:hep-ex/9912017].

[15] V. M. Abazov *et al.* [D0 Collaboration], Phys. Rev. Lett. **87** (2001) 251805 [arXiv:hep-ex/0106026].

[16] D. Acosta *et al.* [CDF Collaboration], Phys. Rev. D **65** (2002) 112003 [arXiv:hep-ex/0201004].

[17] D. Acosta *et al.* [CDF Collaboration], Phys. Rev. D **70** (2004) 074008 [arXiv:hep-ex/0404022].

[18] P. Aurenche, T. Binoth, M. Fontannaz, J.-P. Guillet, G. Heinrich, E. Pilon and M. Werlen, http://lappweb.in2p3.fr/lapth/PHOX_FAMILY/main.html, http://lappweb.in2p3.fr/lapth/PHOX_FAMILY/jetphox.html

[19] P. Aurenche, A. Douiri, R. Baier, M. Fontannaz and D. Schiff, Phys. Lett. B **140** (1984) 87; P. Aurenche, R. Baier, M. Fontannaz and D. Schiff, Nucl. Phys. B **297** (1988) 661.

[20] L.E. Gordon and W. Vogelsang, Phys. Rev. D **50** (1994) 1901.

[21] F. Aversa, P. Chiappetta, M. Greco and J.Ph. Guillet, Nuc. Phys. B **327** (1989) 105; P. Aurenche, P. Chiappetta, M. Fontannaz, J.Ph. Guillet and E. Pilon, Nuc. Phys. B 399 (1993) 34.

[22] H. Baer, J. Ohnemus and J. F. Owens, Phys. Lett. B **234** (1990) 127; Phys. Rev. D **42** (1990) 61

[23] L. E. Gordon and W. Vogelsang, Phys. Rev. D **52** (1995) 58.

[24] E. Laenen, G. Oderda and G. Sterman, Phys. Lett. B **438** (1998) 173 [arXiv:hep-ph/9806467].

[25] S. Catani, M.L. Mangano, P. Nason, JHEP **9807** (1998) 024.

[26] S. Catani, M.L. Mangano, P. Nason, C. Oleari, W. Vogelsang, JHEP **9903** (1999) 025 [arXiv:hep-ph/9903436].

[27] N. Kidonakis, J.F. Owens, Phys. Rev. D **61** (2000) 094004 [arXiv:hep-ph/9912388].

[28] G. Sterman and W. Vogelsang, JHEP **0102** (2001) 016 [arXiv:hep-ph/0011289].

[29] D. de Florian and W. Vogelsang, Phys. Rev. D **72** (2005) 014014 [arXiv:hep-ph/0506150].

[30] G. Sterman and W. Vogelsang, Phys. Rev. D **71** (2005) 014013 [arXiv:hep-ph/0409234].

[31] S. Catani, M. Fontannaz, J.-P. Guillet and E. Pilon, JHEP **0205** (2002) 028 [hep-ph/0204023].

[32] M.A. Furman, Nucl. Phys. B **197** (1982) 413; W.T. Giele and E.W.N. Glover, Phys. Rev. D **46** (1992) 1980; W.T. Giele, E.W.N. Glover and D.A. Kosower, Nucl. Phys. B **403** (1993) 633; P. Chiappetta, R. Fergani and J. P. Guillet, Phys. Lett. B **348** (1995) 646; Z. Phys. C **69** (1996) 443.

[33] R.K. Ellis, D.A. Ross and A.E. Terrano, Nucl. Phys. B **187** (1981) 421; S. Frixione, Z. Kunszt and A. Signer, Nucl. Phys. B **467** (1996) 399; S. Catani and M.H. Seymour, Nucl. Phys. B **485** (1997) 291.

[34] Z. Belghobsi, M. Fontannaz, J.-P. Guillet, G. Heinrich and M. Werlen, in preparation.

[35] J. Pumplin, D. R. Stump, J. Huston, H. L. Lai, P. Nadolsky and W. K. Tung, JHEP **0207** (2002) 012 [arXiv:hep-ph/0201195].

[36] L. Bourhis, M. Fontannaz and J. P. Guillet, Eur. Phys. J. C **2** (1998) 529 [arXiv:hep-ph/9704447].

[37] A.D. Martin, R.G. Roberts,W.J. Stirling, R.S. Thorne, Phys. Lett. B **604** (2004) 61 [arXiv:hep-ph/0410230]

[38] A. Aktas *et al.* [H1 Collaboration], Eur. Phys. J. C **38** (2005) 437 [arXiv:hep-ex/0407018].

[39] P. Aurenche, M. Fontannaz, J. P. Guillet, B. A. Kniehl, E. Pilon and M. Werlen, Eur. Phys. J. C **9** (1999) 107 [arXiv:hep-ph/9811382].

[40] M. Werlen *et al.* [UA6 Collaboration], Phys. Lett. B **452** (1999) 201.

[41] J. Huston, E. Kovacs, S. Kuhlmann, H.L. Lai, J.F. Owens and W.K. Tung, Phys. Rev. **D51** (1995) 6139.

[42] U. Baur *et. al.* (2000) [arXiv:hep-ph/0005226].

[43] W. Vogelsang and A. Vogt, Nucl. Phys. B **453** (1995) 334 [arXiv:hep-ph/9505404].

[44] The DØ Collaboration, DØ note 4751-CONF, http://www.do.fnal.gov

[45] A. Abulencia *et.al.* [CDF Collaboration] [arXiv: hep-ex/0512020]
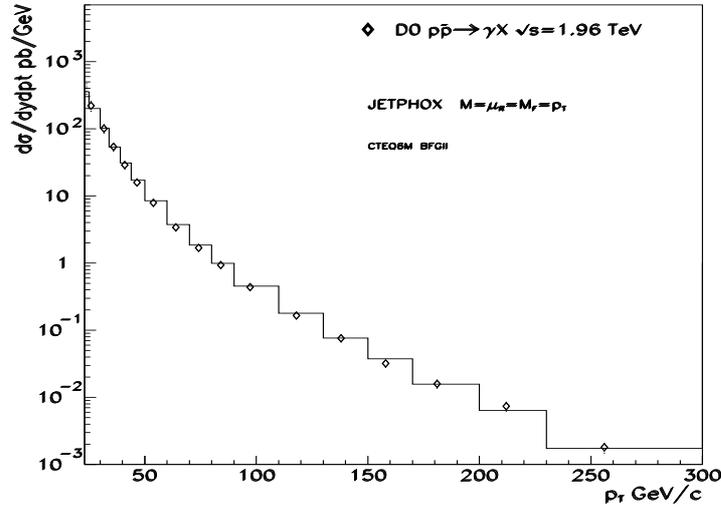
Figure 1: The isolated D∅ photon cross section in the central ($|\eta| < .9$) pseudorapidity region. The histogram is the NLO QCD prediction discussed in the text. The errors are the sum of the statistical and systematic errors. The scales are $\mu = p_T$.
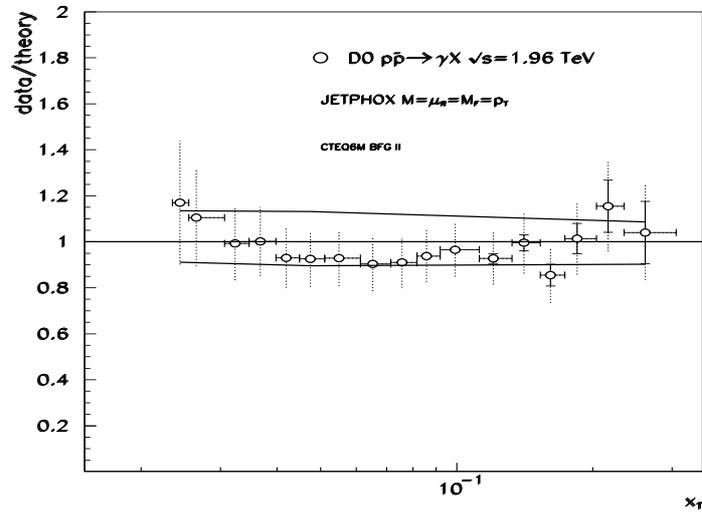
Figure 2: The ratio of D∅ data to NLO QCD obtained with $\mu = p_T$. Ratios of the predictions for $\mu = p_T/2$ ($\mu = 2p_T$) to the nominal theory ($\mu = p_T$) are shown by the upper curve (lower curve).
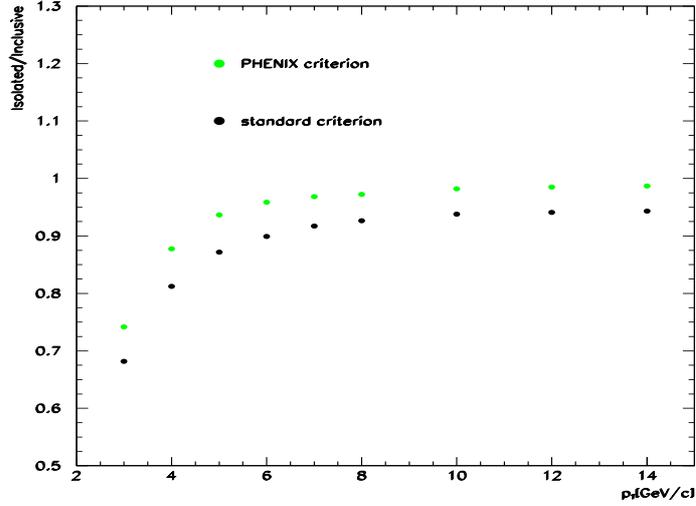
Figure 3: Ratio $\sigma^{th\,isol}/\sigma^{th\,incl}$ of the NLO isolated cross sections to the NLO inclusive prompt-photon cross sections at $\sqrt{s} = 200$ GeV. The scales used are $\mu = p_T/2$. PHENIX criterion: colored dots; standard criterion: black dots
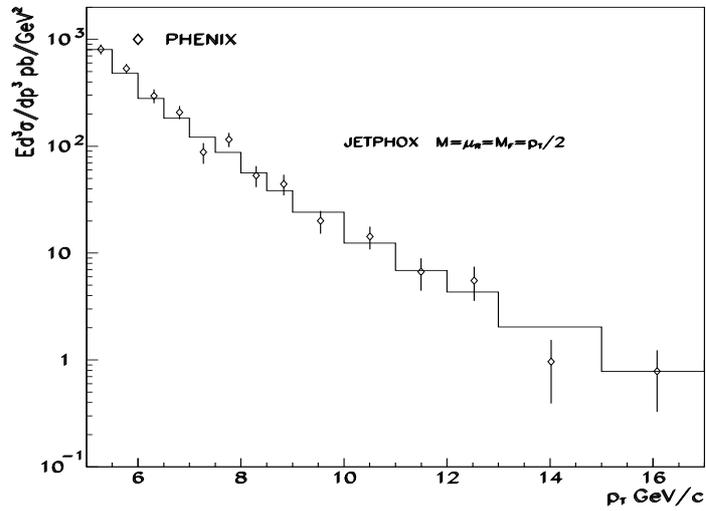
Figure 4: The PHENIX isolated prompt-photon cross section at $\sqrt{s} = 200$ GeV compared with NLO cross section predictions. Only the statistical errors on the data are shown. The scales used in the theoretical calculation are $\mu = p_T/2$.

13
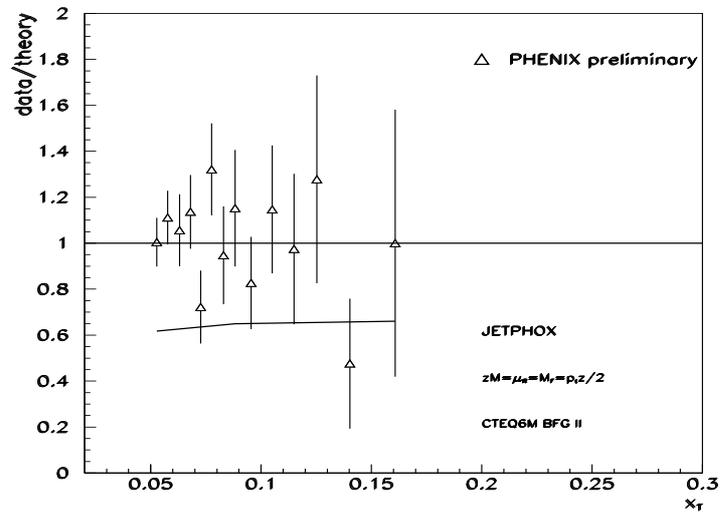
Figure 5: The ratio of PHENIX isolated photon data to NLO QCD using $\mu = p_T/2$. The lower curve corresponds to the ratio $\mathrm{NLO}(2p_T)/\mathrm{NLO}(p_T/2)$. Only the statistical errors on the data are shown.
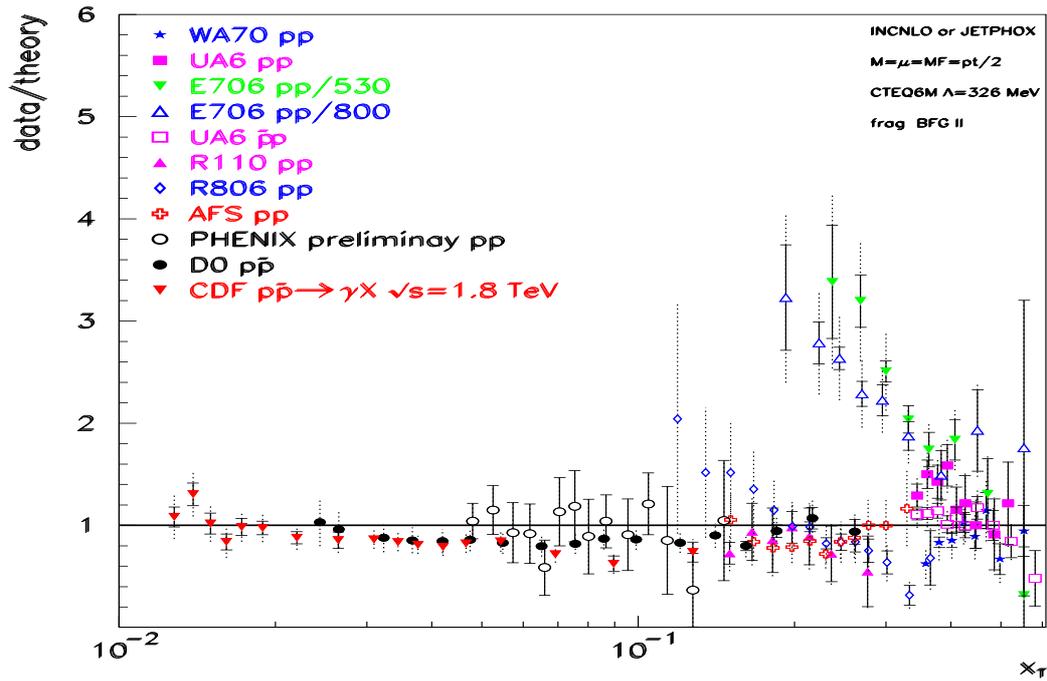
Figure 6: Ratios data/theory for collider and fixed target data with the scale $\mu = p_T/2$. For PHENIX and lower energy data the inclusive cross section is used while the isolated one is used for CDF and D∅. Statistical erros only for PHENIX data.
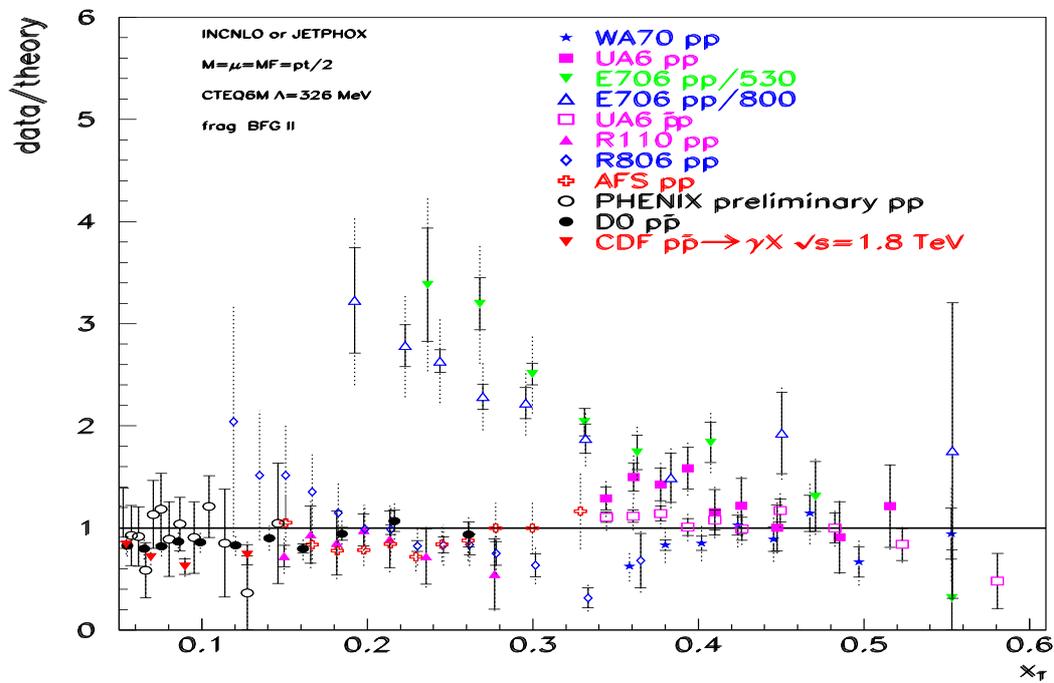


Figure 7: Zoom on the large x_T data with a linear scale in x_T.
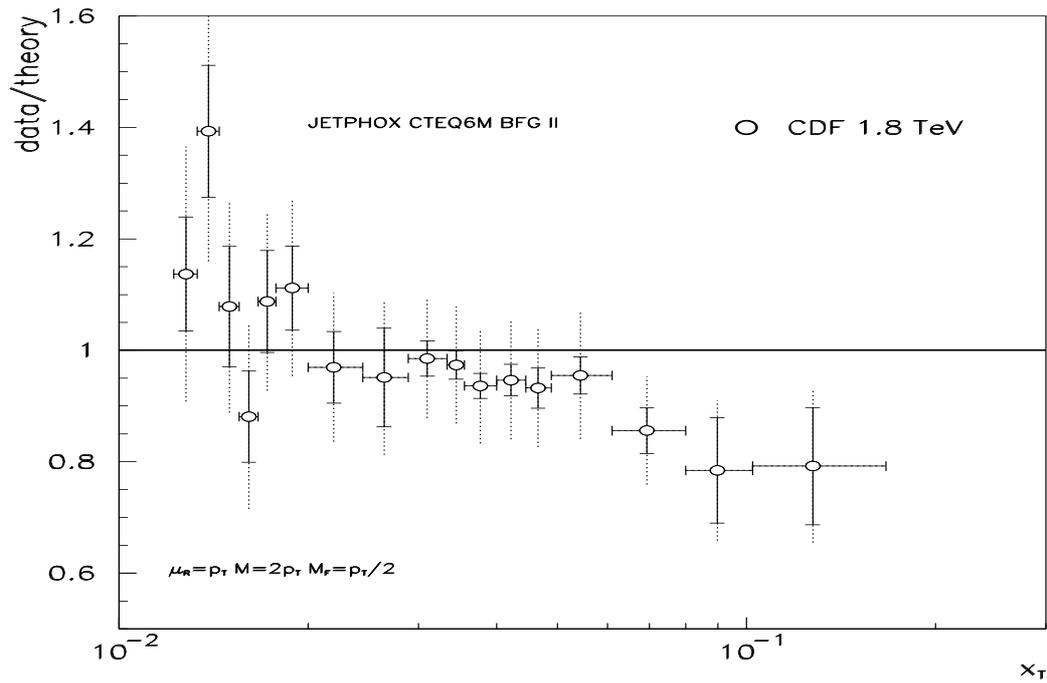
Figure 8: CDF data versus theory for the choice of scales as shown in the figure.
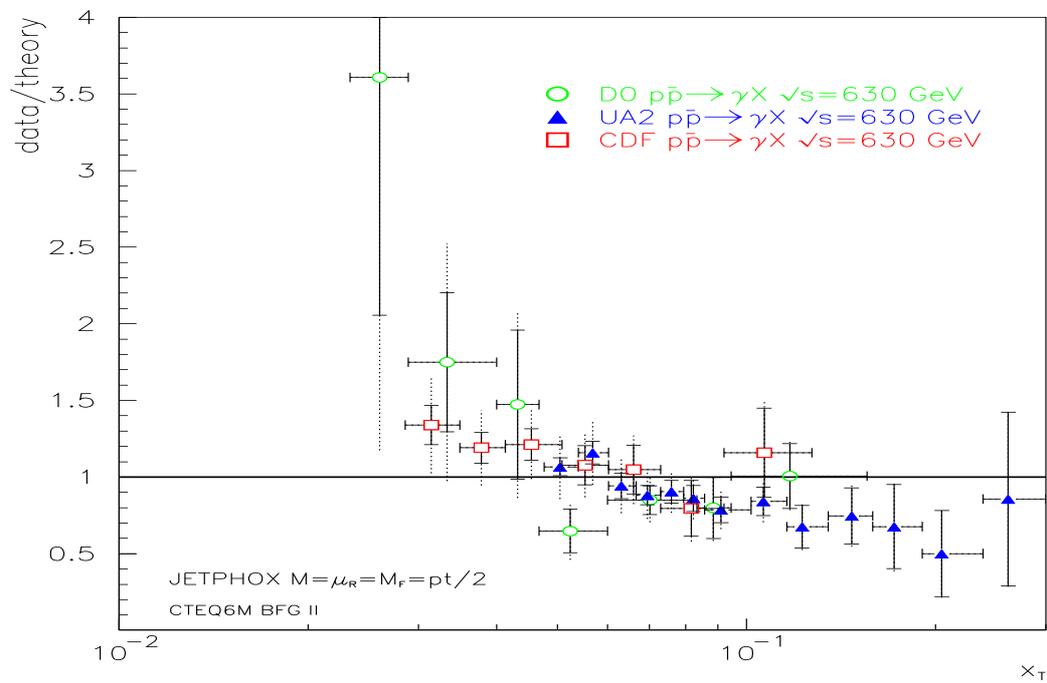
Figure 9: Ratios data/theory for collider data at $\sqrt{s} = 630$ GeV. The scales are $\mu = p_T/2$.
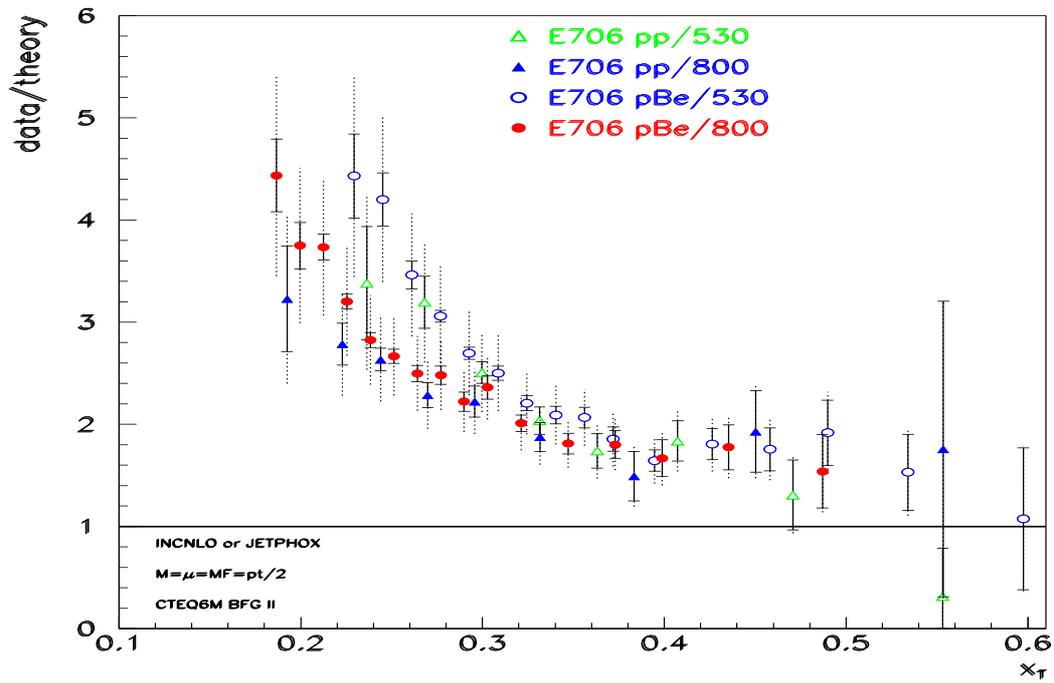
Figure 10: Comparison of pp and pBe data of E706 normalised by the theoretical predictions with scales $p_T/2$.

17

JETPHOX

$M=\mu_R=M_F=p_T/2$

$E d^3\sigma/dp^3$ pb/GeV^2

p_T GeV/c

- D0 p$\bar{\text{p}}$ √s=1.96 TeV
- CDF p$\bar{\text{p}}$ √s=1.8 TeV
- D0 p$\bar{\text{p}}$ √s=630 GeV
- CDF p$\bar{\text{p}}$ √s=630 GeV
- UA2 p$\bar{\text{p}}$ √s=630 GeV
- PHENIX pp 200 GeV prelim.
- AFS pp √s=63 GeV
- R110 pp
- R806 pp
- E706 pp √s=38.8 GeV
- E706 pp √s=31.6 GeV
- UA6 $\bar{\text{p}}$p
- UA6 pp √s=24.3 GeV
- WA70 pp √s=22.9 GeV

$*10^{-4}$
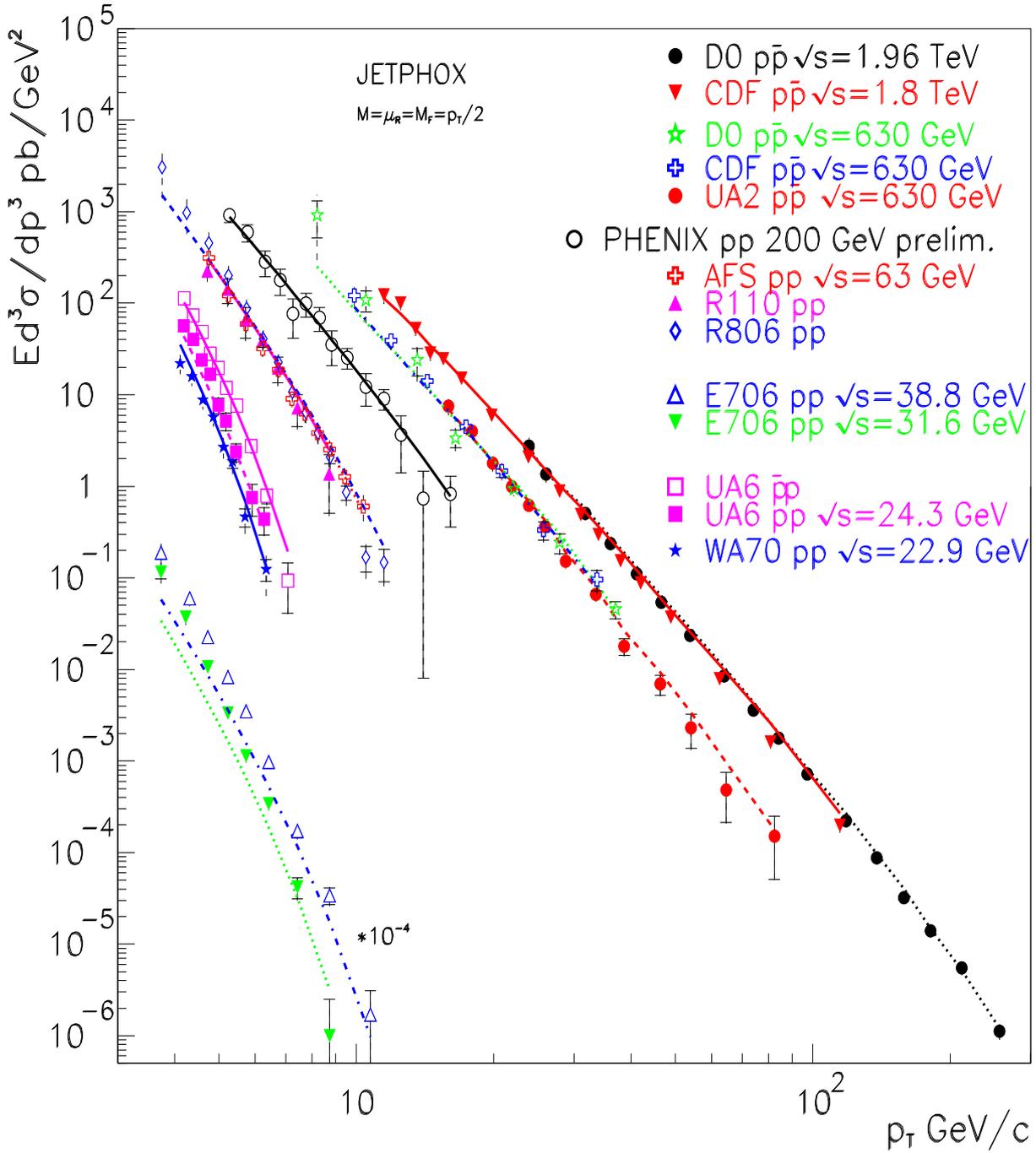
Figure 11: World's inclusive and isolated direct photon productions cross sections measured in proton-proton and antiproton-proton collisions compared to JETPHOX NLO predictions using BFG II (CTEQ6M) for fragmentation (structure) functions and a common scale $p_T/2$. For the clarity of the figure the E706 data are scaled by a factor 10^{-4}.

18
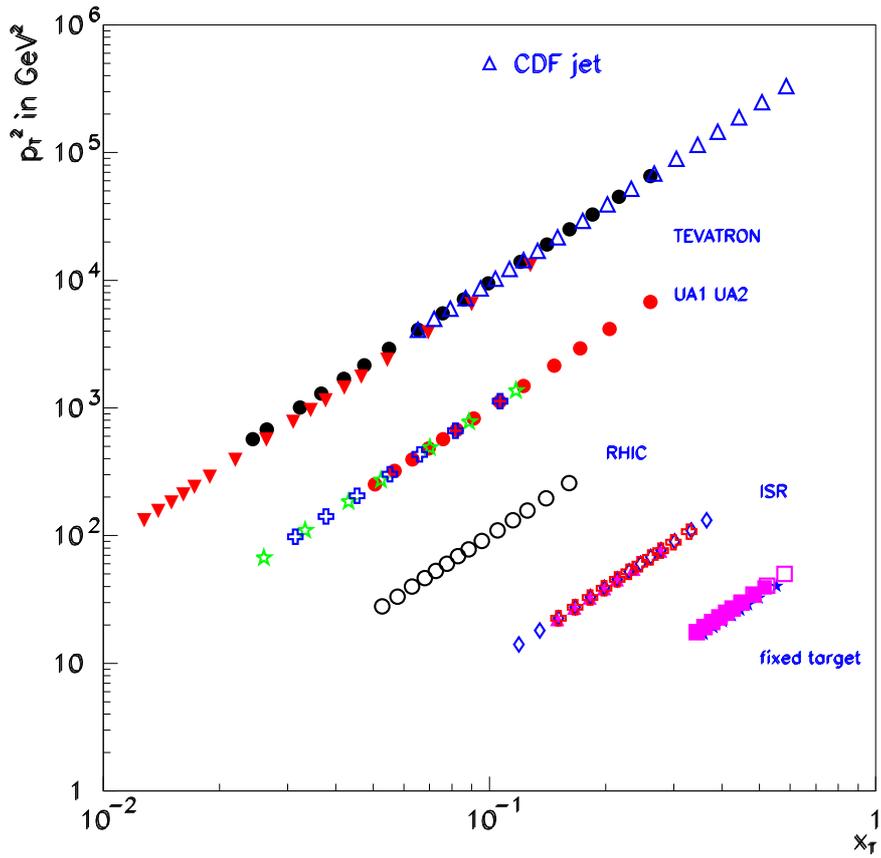
Figure 12: The kinematical region probed by prompt photon experiments compared to that relevant for jet production. Each data point is represented by a symbol as in Fig. 11 for photons, and by open triangles for jets.